A&A 378, 735–739 (2001)
DOI: 10.1051/0004-6361:20011271

Astronomy & Astrophysics

Small-scale fluctuations of the soft X-ray background

A. Sołtan[1], M. J. Freyberg[2], and J. Trümper[2]

[1] Nicolaus Copernicus Astronomical Center, Bartycka 18, 00-716 Warsaw, Poland
[2] MPI für extraterrestrische Physik, Giessenbachstr., 85748 Garching, Germany
e-mail: mjf@mpe.mpg.de (MJF); jtrumper@mpe.mpg.de (JT)

Received 1 June 2001 / Accepted 6 September 2001

Abstract. We report the detection of the X-ray background fluctuations at small angular scales. *ROSAT* PSPC archive pointed observations are used to measure the autocorrelation function (ACF) of the background at scales of $0\overset{\circ}{.}03-0\overset{\circ}{.}3$. The pointings have been selected from an area apparently free from galactic contamination and the ACF signal is generated mostly by the extragalactic component of the XRB. At separations below $\sim 0\overset{\circ}{.}1$ known X-ray clusters of galaxies become a substantial source of the background fluctuations. Assuming a power law, the ACF for all the data has a slope of $\sim$1, but is substantially flatter (with slope of $\sim$0.6) when pointings containing bright clusters are removed. Flattening of the ACF at small separations could indicate existence of a hot, nonuniformly distributed gas accumulating in wells of gravitational potential. At separations $0\overset{\circ}{.}3-0\overset{\circ}{.}4$ where the ACF estimates based on the *ROSAT* pointings and All-Sky Survey are available, both data sets give consistent results.

Key words. X-rays: general – diffuse radiation

1. Introduction

Fluctuations of the X-ray background (XRB) provide unique information on its constitution. Although the soft X-ray background (XRB) is dominated by discrete sources (Lehmann et al. 2001 and references therein), the distinct diffuse thermal component is also present. Investigating the XRB spectrum Hasinger (1992) detected a thermal emission by galactic plasma. Nonuniform spatial distribution within the Galaxy of the emitting gas introduces pronounced anisotropy to the XRB. Diffuse emission of extragalactic origin is also predicted. Hydrodynamic computations by Cen & Ostriker (1999) show that the process of accumulation of primordial gas in the potential wells created by galaxies and clusters of galaxies has produced large scale concentrations of hot plasma. This material is expected to emit thermal bremsstrahlung in the soft X-ray domain. A clumpy distribution of emitting plasma would contribute substantially to the total fluctuations of the XRB.

At angular scales above $\sim 0\overset{\circ}{.}3$ the *ROSAT* All-Sky Survey (RASS) revealed distinct variations of the soft XRB (Sołtan et al. 1996). For the description of *ROSAT* see Trümper (1983) and for the RASS – Snowden & Schmitt (1990). In the first attempt to measure the ACF using the *ROSAT* pointings Sołtan & Hasinger (1994) have obtained the upper limits substantially below the ACF measurement derived later from the RASS. This apparent disagreement resulted from two reasons. First, Sołtan & Hasinger (1994) have a priori assumed that the XRB fluctuations at separations larger than the effective pointing field of view are negligible. Second, in their calculations of the ACF all the discrete sources detected in each pointing have been removed, which reduced the ACF amplitude still further (Sliwa et al. 2001, in preparation).

Subsequent analysis (Sołtan et al. 1999) showed that clustering of active galactic nuclei potentially could explain the large amplitude of the XRB autocorrelation function (ACF). However, the amplitude of X-ray source spatial clustering required to reproduce the observed ACF is higher than that derived from direct investigation of the distribution of sources (e.g. Carrera et al. 1998). Thus, it is likely that fluctuations of the soft XRB observed in RASS are partially produced also by galactic and extragalactic plasma. To evaluate contribution of different sources to the XRB anisotropies one needs to measure the amplitude of the XRB fluctuations over a wide range of angular separations and at different energies. In the present work we have determined the autocorrelation function of the soft XRB at small angular scales using a large number of *ROSAT* pointings. Below we describe the observational material used in the analysis, the computational details and compare the present results with our earlier measurements of the ACF at large separations using the RASS.

Send offprint requests to: A. Sołtan,
e-mail: soltan@camk.edu.pl

2. Analysis of the observational data

Observational material used in the investigation of the background anisotropy should satisfy stringent criteria of homogeneity. It has been shown that at large angular scales the RASS is well suited for that purpose (e.g. Sołtan et al. 1997, 1999). Using a large section of the RASS they determined the amplitude of the autocorrelation function of the XRB at separations between $0\overset{\circ}{.}4$ and $\sim 10^\circ$. At larger distances the XRB fluctuations drop below the statistical noise and (possibly) the systematic residual errors not removed in the process of data reduction. Small separation limit results from the pixel size of the RASS maps. The final RASS data are binned into $12' \times 12'$ pixels roughly corresponding to area of the 90% integral of the effective survey point spread function.

The angular resolution of the X-ray mirror/PSPC system – particularly in the central zone of the field of view – is much better than this limit and allows for the fluctuation analysis down to separation of $2'-3'$. Thus, the *ROSAT* pointed observations could be used to extend our measurements of the XRB variations to small scales. Although the *ROSAT* telescope full field of view has a diameter of almost 2°, only the area within the central ring of the PSPC window supporting structure can be effectively used in the present investigation. Beside the high angular resolution, this area is subject least to the vignetting effect and constitutes the largest contiguous section of the field of view. During the pointed observation the satellite makes small oscillations around the nominal pointing direction, what further reduces the non obstructed area. In effect, central region of just $13'-14'$ radius is uniformly illuminated by the cosmic X-rays.

The area of the individual *ROSAT* pointing suitable for the anisotropy study is too small to give accurate estimates of the XRB fluctuations. Smooth extrapolation of the RASS autocorrelation function to separations of $\sim 0\overset{\circ}{.}2$ gives the amplitude of the order of 0.02 while typical estimates of the ACF based on a single pointing have uncertainties of the order of 0.1 (see Fig. 1).

To reduce statistical scatter resulting from a small number of photons, we utilized a large number of *ROSAT* observations. The archived observational material has been searched and a sample of pointings satisfying selection criteria was constructed.

The objective of the present investigation was to determine the anisotropy of the *extragalactic* component of the XRB. The RASS X-ray maps (Snowden et al. 1997) show that at low energies only the selected sky regions seem to be free from thermal emission by hot galactic plasma and not affected by absorption by cold gas. To minimize effects of the Galaxy, Sołtan et al. (1996) used a section of the RASS maps of approximately 1 sr at the northern galactic hemisphere ($b > 40^\circ, 70^\circ < l < 250^\circ$) apparently least contaminated by local effects. In the present analysis we have concentrated on the same region of the sky. The data in the gain-corrected pulse height channels 91−131 ("R6 band" in Snowden et al. 1994) with the energy

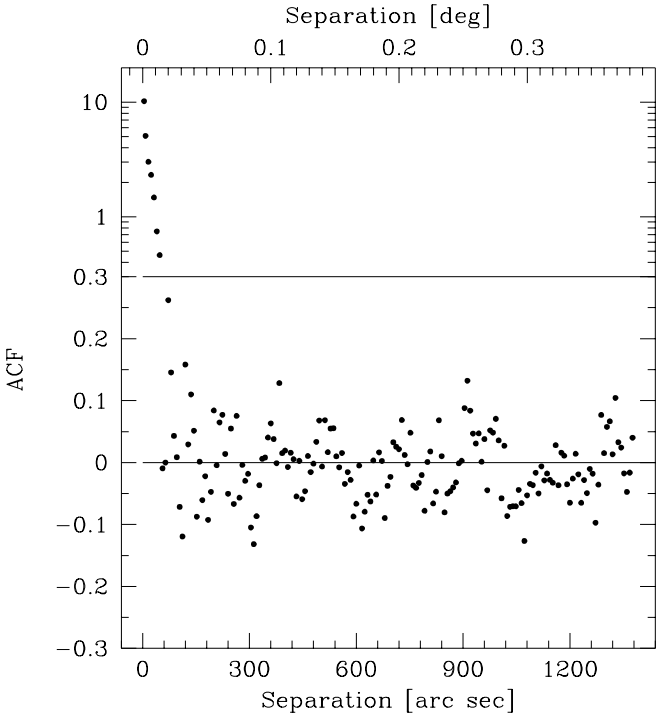

Fig. 1. An example of the autocorrelation function based a single pointing of 10 800 s; note the change of scale from linear to logarithmic in the ordinate.

centered at 1.15 keV have been selected. All *ROSAT* pointed observations within this area and exposure times longer than 5000 s have been examined. First, pointings at known extended sources (supernova remnants, nearby normal galaxies, clusters and groups of galaxies) have been excluded. Most of the remaining pointings are centered on either galactic stars or distant AGNs. Many of these sources are bright and due to wide wings of the point spread function they contribute noticeable counts at large angular separations from the source centroid position. The distribution of counts in the field of view generated by each target source according to the point spread function was calculated. Areas in which the local contribution by the target source exceeded 5% of the average background in the field have been removed from further analysis. Thus, the residual relative fluctuations produced by target sources are smaller than 0.05 in the selected data and this value defines the detection threshold for the cosmic variation of the background in the present investigation.

In the *ROSAT* archive there are 143 PSPC pointings satisfying all the criteria. In Fig. 2 the distribution of these pointings in the celestial sphere is shown. Although observations are distributed non randomly, the area in question is covered by pointings roughly uniformly. This indicates that statistical estimates based on the available sample of pointings should be representative for the whole area.

2.1. Data homogeneity

Of 143 pointings shown in Fig. 2 142 have been acquired between July 1990 and April 1994 and one observation in

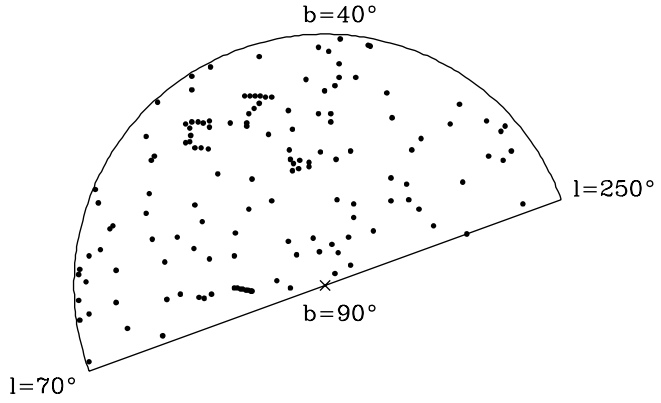

Fig. 2. Distribution of 143 *ROSAT* PSPC pointings used in the investigation; labels locate the area in galactic coordinates. Dots representing pointings are not drawn to scale.

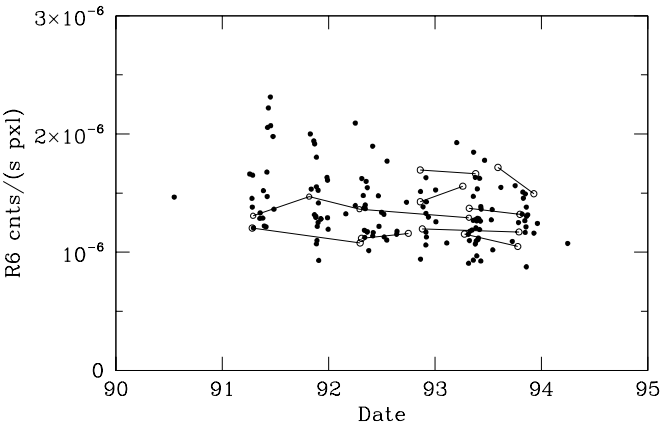

Fig. 3. Average count rate per pixel recorded in the R6 band as a function of time. Open symbols connected with lines show observations of the same pointing.

February/March 1997. Stability of the PSPC performance has been monitored routinely during the entire satellite operation. Nevertheless, over such long period of time systematic drift of telescope characteristics could not be excluded. To assess possible variations of the instrument parameters we have plotted in Fig. 3 the average count rate in each field (excluding the target source) vs. time of the observation. For 9 pointings individual observations were separated by several months or years and these are shown with open circles. All the observations were carried out with the PSPC detector B except that made in July 1990 when PSPC C was used. To minimize variations resulting from instrumental effects, this observation and that of 1997 have not been used in the subsequent data analysis. The final sample contains 141 pointings accumulated between April 1991 and April 1994. Apart from the large scatter of the average count rate between observations, there seems to be a systematic trend with time. The effect is weak and difficult to evaluate statistically. Nevertheless, observations of the same pointings also indicate some systematic decline of the detected count rates, although its statistical significance is questionable. In our calculation

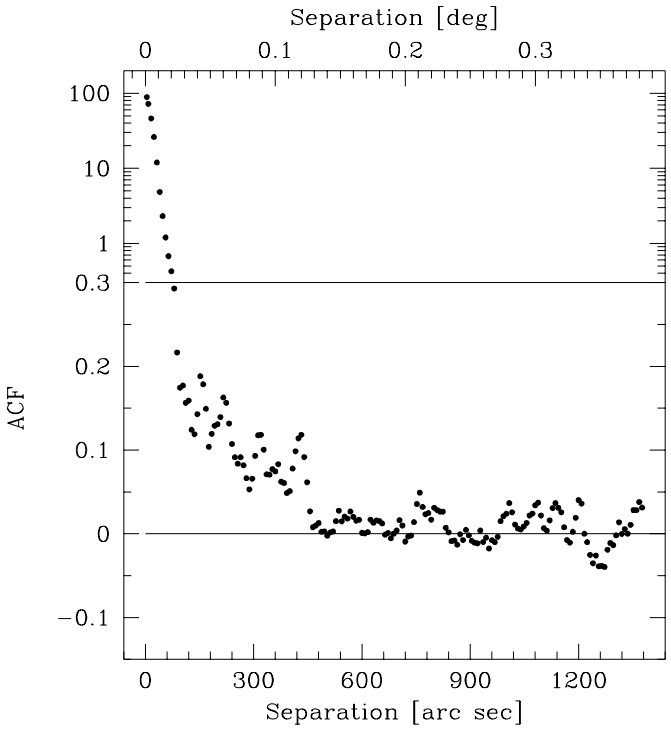

Fig. 4. The autocorrelation function for the whole sample of 141 pointings.

of the autocorrelation function we take this possible trend into account (see below).

3. The autocorrelation function

The autocorrelation function is estimated using standard definition:

$$w(\theta) = \frac{1}{\langle\rho\rangle^2}\,\frac{1}{n_{\rm p}(\theta)}\sum_{i,j}\rho(i)\rho(j)_{|\theta} - 1, \qquad (1)$$

where $\langle\rho\rangle$ denotes the average count rate per pixel, $\rho(i)$ is the count rate in the ith pixel, the sum extends over all pixel pairs separated by the angle θ, and $n_{\rm p}(\theta)$ is the number of these pixel pairs.

It is assumed that our observations constitute a fair sample of the XRB. Although observations differ substantially with respect to exposure time, all the pointings enter our calculations with equal weights. The noise of the ACF amplitude estimate is generated mostly by pairs of X-ray sources rather than the photon counting statistics.

The ACF calculated according to Eq. (1) using all the 141 pointings is shown in Fig. 4.

3.1. Bright source problem

Fluctuations of the XRB at the smallest scales are dominated by the discrete nature of the background. Bright sources produce sharp peak in the ACF with characteristic width defined by the point spread function. At larger separations the ACF signal is subject to fluctuations produced mainly by the source pairs. Because the number of

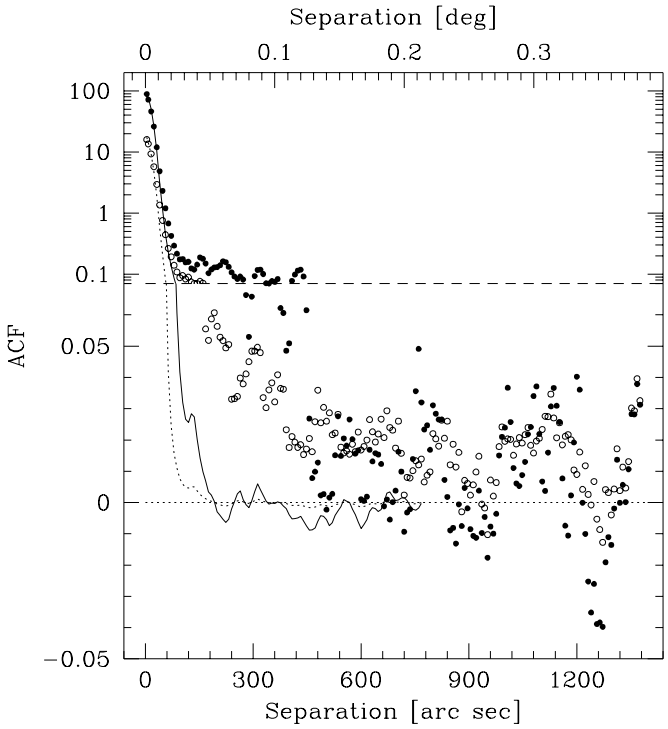

Fig. 5. The autocorrelation function for the whole sample (same as Fig. 4) – full symbols, and for the sample without the pointing which contains the strongest source in the sample – cluster of galaxies A 1774 – open circles. Solid and dotted curves – the ACFs expected for the population of point sources in those samples (see text).

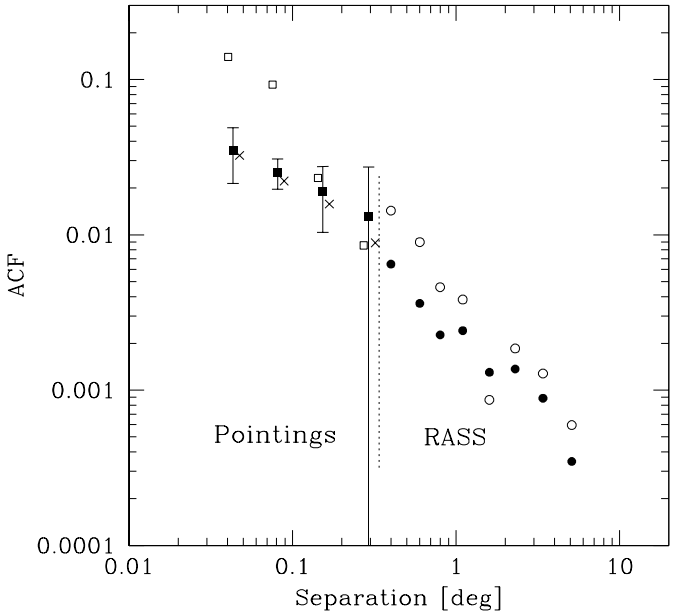

Fig. 6. Autocorrelation functions based on the *ROSAT* pointings and the All-Sky Survey. Pointings: open squares – the ACF in the whole sample (same as in Fig. 4); full squares – the ACF based on pointings without bright sources associated with known clusters of galaxies; crosses – the ACF corrected for "date effect" (see text). For clarity some points have been slightly displaced. RASS: open circles – the ACF of all the data; full circles – the ACF based on data without pixels of the highest count rate (see text).

sources in the present sample is large, fluctuations of the ACF are relatively weak, although easily visible. Effects of individual strongest sources on the ACF are illustrated in Fig. 5, where we plotted the ACF based on all the pointings (same as Fig. 4) and the ACF without the field containing the strongest source in the whole sample – the cluster of galaxies A1774. Centrally peaked source coinciding with the cluster is surrounded by extended emission of $\sim 7'$ diameter. This entire structure contributes significantly to the ACF signal at small angles. At larger separations it increases substantially the noise but does not affect significantly the average signal.

Effects of the point spread function (PSF) are examined in the following way. A large number of observations directed at bright point like galactic sources have been used to compute the template ACF. In this case virtually all the ACF signal is generated by the PSF and is concentrated in the peak produced by individual sources. This template ACF has been scaled to match the observed ACFs at separations corresponding to the width of the central PSF peak and is shown with the solid and dotted curves in Fig. 5. The model ACF indicates the contribution to the observed ACFs due to the finite width of the PSF. It is evident that at separations greater than $1'.5-2'$ the ACF amplitude produced by wings of the PSF is negligible in comparison to the observed signal.

3.2. Known extended sources

Fields used in our ACF calculations have been selected from observations directed either at point sources or without known bright sources at all, usually the deep exposures aimed to study the XRB. Nevertheless, serendipitous sources associated with known clusters of galaxies have been found within the field of view of several pointings. It appears that a substantial fraction of the ACF amplitude at small separations is generated by these objects. To assess this effect we have removed from the sample 11 pointings with conspicuous extended sources associated with clusters. The ACF computed using fields without bright clusters is shown in Fig. 6 together with the ACF from the entire sample. Error bars representing $1\,\sigma$ uncertainties for the ACF of the "no cluster" sample have been estimated as follows. The pointings have been divided into six roughly equal size groups and the ACF has been calculated for each subsample separately. Scatter between ACFs was used to estimate the uncertainty of the average result based on the entire sample. These errors account for both the cosmic variance related to the large scale effects and local statistical fluctuations. Although the error bars are large and do not provide restrictive constraints on the ACF slope below $0^{\circ}.2$, our results suggest flattening of the ACF at the small separation limit. It is evident that removal of known cluster sources affects mainly the ACF at the smallest separations (below $\sim 0^{\circ}.1$). In this range roughly 75% of the ACF amplitude is produced by known

clusters, while at larger distances the effect is lost in the statistical noise.

3.3. Instrumental effects

Systematic instrumental effects which are revealed by the apparent correlation between the average count rate and the time of observation shown in Fig. 3 generate artificial ACF signals. The magnitude of this effect has been estimated assuming that there is a linear trend of the effective instrument sensitivity with time. Using the regression line the observed count rates in each field were reduced to a single epoch and the calculations of the ACF have been repeated. This procedure yields the ACF amplitude lower by 0.003−0.004 than for the raw data. In Fig. 6 the corrected ACF for cluster free sample is shown with crosses.

3.4. Comparison with RASS

The largest angular scale effectively accessible for the *ROSAT* pointings does not overlap with scales of the *ROSAT* All-Sky Survey, but both observational modes meet at about 0.°3−0.°4. Nevertheless, the comparison of the present results with the RASS data is not straightforward. In the selection procedure of our sample from the *ROSAT* archive all the observations of bright or extended sources have been discarded. Since the *ROSAT* target list contained a great number of such sources, the present sample is biased against certain classes of object which potentially could produce a strong ACF signal.

Contribution of bright sources to the ACF amplitude is visible in the RASS. In Fig. 6 we plot with open circles the ACF based on the RASS from the whole area considered in the analysis (Fig. 2); solid circles show the ACF computed from the same region after 1% of pixels with the highest count rate have been removed. At separations below 1° both ACFs differ by a factor of ∼2. Taking this effect into consideration one may conclude that the apparent agreement at ∼0.°35 between the ACF amplitudes derived from pointings and RASS is satisfactory, but full description of the XRB fluctuations requires more detailed investigation.

4. Conclusions

The ACF calculated from the *ROSAT* pointings is consistent with the extrapolation of the ACF derived from the RASS. It seems that relatively steep slope of the ACF at small separations is produced by X-ray clusters of galaxies. Our "best estimate" of the ACF without bright clusters is shown with crosses in Fig. 6. Slope of this relationship below 0.°2 is equal to 0.6 and is smaller than the "canonical" value of 0.7−0.8. If this discrepancy is confirmed by more accurate determinations, it would imply that the XRB fluctuations at these angular scales are not generated by standard clustering of X-ray sources described by the 3D correlation function with the slope of 1.8. Flat slope of the ACF could indicate that some XRB variations are associated with the emission by hot extragalactic plasma distributed in clumps according to the Cen & Ostriker (1999) model.

Acknowledgements. The ROSAT project is supported by the German Bundesministerium für Bildung und Forschung/Deutsches Zentrum für Luft- und Raumfahrt (BMBF/DLR) and by the Max-Planck-Gesellschaft (MPG). The authors thank the referee Dr. Omar Almaini for his critical and constructive attitude to their work. This paper was supported by the Polish KBN grant 5 P03 D 022 20.

References

Carrera, F. J., Barcons, X., Fabian, A. C., et al. 1998, MNRAS, 299, 229
Cen, R., & Ostriker, J. P. 1999, ApJ, 514, 1
Hasinger, G. 1992, *ROSAT* Deep Surveys, in Proc. MPE Conf., X-ray Emission from Active Galactic Nuclei and the Cosmic X-ray Background, ed. W. Brinkmann, & J. Trümper (MPE, Garching)
Lehmann, I., Hasinger, G., Schmidt, M., et al. 2001 [astro-ph/0103368]
Snowden, S. L., McCammon, D., Burrows, D., et al. 1994, ApJ, 424, 714
Snowden, S. L., Egger, R., Freyberg, M. J., et al. 1997, ApJ, 485, 125
Sołtan, A. M., Freyberg, M., Hasinger, G., et al. 1999, A&A, 349, 354
Sołtan, A. M., & Hasinger, G. 1994, A&A, 288, 77
Sołtan, A. M., Hasinger, G., Egger, R., Snowden, S., & Trümper, J. 1996, A&A, 305, 17
Sołtan, A. M., Hasinger, G., Egger, R., Snowden, S., & Trümper, J. 1997, A&A, 320, 705
Snowden, S. L., & Schmitt, J. H. M. M. 1990, Ap&SS, 171, 207
Trümper, J. 1983, Adv. Space Res., 4, 241